SSRG International Journal of Civil Engineering
ISSN: 2348-8352/ https://doi.org/10.14445/23488352/IJCE-V12I9P104

Volume 12 Issue 9, 37-48, September 2025

Original Article

Advanced Prestressing Strategies for Curved Spans in Segmental Bridges: A Comprehensive Procedure for Segmental Bridge Design and Analysis

N. J. Jain[1], S. Sangita Mishra[2], Shrikant Charhate[3]

[1,2,3]*Amity School of Engineering and Technology, Amity University, Mumbai, Maharashtra, India.*

[1]*Corresponding Author : nilesh.jain108@gmail.com*

Received: 05 July 2025 Revised: 06 August 2025 Accepted: 04 September 2025 Published: 29 September 2025

Abstract *- The analysis and design of post-tensioned composite concrete segmental bridge structures represent significant challenges because of their complex geometric arrangement and their highly challenging construction requirements. Conventionally adopted practices for the design of such bridge structures often struggle to address the core issues, such as tendon profile, anchorage zones and the stress distribution in the large curved spans, where any minor anomaly or error that occurs during the on-site execution may lead to a catastrophic structural failure. Key aspects involved are the assessment of tendon layouts or profiles, anchor zones and the stress distribution under the diverse loading conditions to ensure optimal structural performance and stability. To overcome these limitations, this study conducts a detailed parametric investigation into the influence of curvature radius, high tensile tendon profiles, and jacking force on the structural response of curved bridge spans. An advanced Finite Element Analysis Method (FEAM) was employed to evaluate the performance and to compare the conventional design and on-site methods with modern practices prescribed by the Indian Standard Codes (IS), Indian Roads Congress (IRC) and Ministry of Road Transport and Highways (MoRTH) specifications. Under the exceptional conditions, the maximum allowable overstressing observed during the prestressing operations is 95% of 0.1% proof load or proof stress, which is almost 0.826 times the Ultimate Tensile Strength (UTS). The results also indicate that the variations in cable lengths between the inner and outer webs can lead to overstressing of the inner web tendon bars by a factor of 1.05 times, increasing the stress variation at the bottom fibre and altering the bending moment distribution across the span. The findings also highlight the critical correlations between the prestressing parameters and the span curvature, offering practical insights for improving the design accuracy and execution of safety in post-tensioned curved bridge structures.*

Keywords *- Curved span, Prestressing, Segmental bridge, Structure behavior, Tendon profile.*

1. Introduction

Prestressing in a curved span of PSC box-type superstructure during the construction phase of segmental bridges is quite a sophisticated engineering technique that plays an important and critical role in ensuring the structural stability, durability, and serviceability of such complex bridge structures. In comparison with the straight spans of the bridge structure, the curved spans need extra attention due to their change in geometry profile, which includes uneven distribution of stresses with higher bending moments and unique load transfer mechanisms. Prestressing of the structure helps to counteract these forces by applying controlled compressive stresses, enabling the structure to withstand the external loads and to minimize the deformation. The process of prestressing requires precise planning, specially in the case of the segmental box type curved spans during the execution, followed by careful design of tendon profiles, accurate application of the jacking forces, and meticulous monitoring during the construction. By adjusting these factors with accuracy, the prestressing not only enhances the performance of curved spans but also extends the lifespan of the structure in terms of durability. It is also necessary to make it a vital practice in modern bridge engineering. For this reason, understanding the suitable prestressing strategies in PSC segmental bridge structures is important to achieve both structural reliability and economic construction. A detailed review of past studies provides useful insights into how these issues have been addressed previously and what further improvements are needed to avoid any under-construction failures. A critical review of the modern-day literature review is based on the fibre optic sensors used to determine the losses in the prestressed concrete structures [1, 2]. The study reveals that the majority of prestress losses occurred within the first three months after casting. Particularly, the findings indicated that the standard code predictions slightly underestimated the actual prestress losses that occur with respect to time. This

suggests a closer alignment with the fibre optic sensor readings using time step methods than the conventional methods for long-term predictions. A considerable knowledge gap was observed for the curved segmental constructions and the existing knowledge regarding accurate estimations of prestress loss mechanisms, particularly during the early age period of the structural behavior, highlighting the need for advanced Modelling approaches to understand the real-world scenario [1]. Another study for prestress losses caught the attention, for the actual losses were significantly higher than those predicted by Eurocode-2, reaching up to 79% of the predicted ultimate prestressing losses. This highlights the influence of manufacturing processes on the beam performance. Further studies also found that the theoretical camber models overestimated field measurements by 32%, highlighting a significant gap between the design assumptions and the actual response of the structure during the construction phase [2]. The literature inadequately captures the effects of time-dependent material behavior (e.g., creep, shrinkage, relaxation) and geometric curvature, emphasising a demand for deep research to ensure the long-term serviceability and safety of the structures [1, 2].

In another study a Discrete Finite Element Model (DFEM) used for analysis of PSC Precast bridge segments to identify the response of structure which concluded that there is and about ±20% of prestressing which lead to an increase of +10% resisting moment and decrease of -16.8% of the moment of resistance which further results into +36.6% and -30.2% of the deflection capacities. However, a critical gap is in understanding the comprehensive effects of prestress losses on long-term effects like concrete shrinkage and creep or maintenance issues [3]. A review related to the prestressed concrete bridges, where several case study examples of the prestressed concrete bridges mainly focus on their design and the practical challenges involved in handling and transportation of precast segments. The study addresses the limitations encountered during the shipping and the prestressing of these bridge segments and discusses the discrete techniques to be used to mitigate such issues effectively [4]. Prestressed concrete segmental bridge construction requires advanced techniques like prestressing, box girder design and the cantilever methods to manage the complex site conditions without any conventional falsework. Key innovations include cast-in-situ and precast segmental construction methods, expanding the practical span length and the adaptability of the concrete bridge structures. These bridges are constructed using methods such as balanced cantilever, span-by-span launching and incremental launching, enhancing their versatility. The evolution of such techniques underscores the importance of the economic feasibility and the adaptability in modern bridge engineering [4, 5]. Further, for the detailed study, it is also essential to explore the core fundamentals of prestressing by performing a finite element-based analysis in order to get an accurate mathematical modelling of the bridge structures. The literature studies based on the Finite Element Analysis (FEA) of reinforced and pretensioned concrete beams utilizing FEA tools to investigate the nonlinear behavior under external loading conditions [6-8]. These studies revealed that the classical reinforced concrete structure theory has accurately predicted the yielding point at about 115.3 kN, with the finite element model indicating the failure in flexure shortly after yielding at a load of 119.58 kN, resulting in maximum deflection of 20.3 mm, as shown in Figure 1 below [8]. Additionally, the analysis showed that the stress curves for the reinforced concrete beam reached an ultimate stress of 25.08 N/mm², while the pre-tensioned beam achieved 40.5 N/mm² [8].

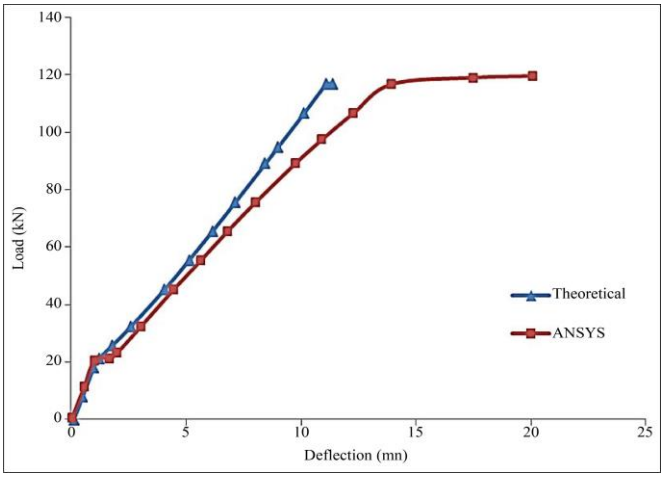

Fig. 1 Load Vs Deflection [8]

However, the researchers acknowledged limitations in modelling structures, particularly regarding the approximations and assumptions made during these stages, which may affect the accuracy of the predictions of stress and strain variations in the prestressing tendon bars. This highlights a gap in the current research, suggesting the need for more refined Modelling techniques to enhance the predictive capabilities of finite element analysis in concrete structures [7, 8]. Another study investigated the effectiveness of various types of prestressing techniques for strengthening Reinforced Concrete (RC) beams, focusing on their impact on structural performance and durability. Key findings indicated that the application of prestressing has significantly enhanced the load-bearing capacity of PSC beams and reduced the deflection, thereby improving their overall structural integrity [9]. This study also highlights the importance of selecting the appropriate prestressing methods, relying on specific loading conditions and the material properties. However, the research does not provide a clear picture, particularly in terms of the long-term performance of the prestressed RC beams under varying site conditions and the economic implications of implementing such techniques in actual practice. Further detailed investigation is needed to develop standardized procedures that can facilitate the detailed adoption of the prestressing methods in the construction industry [9].

A significant research study focuses on developing and validating a nonlinear finite element model to predict the complete structural response of a prestressed concrete bridge, moving beyond simplified and conventionally adopted design methodology. The study is based on the assumption of having a perfect bond between the concrete and the prestressing tendon bars, which limits the model structure's applicability to FRP techniques of strengthening of structure [10]. Another study investigated the effects of long-term creep and prestressing on moment redistribution in balanced cantilever cast-in-situ segmental bridge structures [11, 12]. The researcher's case study for the Pathum Thani bridge reveals the concept that is contrary to the conventional understanding of long-term creep, which can actually increase the magnitude of negative bending moments rather than decreasing them further, highlighting the significant impact of the top cantilever prestressing on the creep redistribution, while the bottom continuity prestressing exhibits minimal/less effect [11]. Further, the findings also suggested that the conventional simplified methods for estimating the long-term bending moments may not accurately explain the increased magnitudes due to prestressing forces. However, the gaps in the study literature are regarding the longitudinal effects of various prestressing configurations on creep, indicating a need for further exploration in this area to refine the existing methodologies in bridge structural analysis [11, 12].

A parametric study investigates the behavior of a PSC box girder with curvature in plan and analyses the effects of curvature angle, prestressing force, compressive strength and tendon profile using the finite element tool. The results concluded that increased curvature leads to a drastic rise in the displacement and the torsional stresses, while tendon elongation remains largely unaffected beyond a prestressing force of 500 kN [13]. The study does not consider losses due to prestressing and the different types of girder, specifically the one with a segmental configuration, which is required for construction in the modern era. Atmaca et al. (2019 determined the maximum span length and the minimum depth for superstructure for prestressed concrete I-girder type bridges by analyzing 12 different girder heights ranging from 60 cm to 180 cm with the spans between 15m and 35m [14]. This study needs further detailed learning for the different girder types and larger spans, considering the prestressing, as the smaller span can be uneconomical for the industrial practices. A case study highlights the significant evolution of prestressing techniques, materials and the advancement in the design philosophy over the past 50 years. Key findings are that the transition towards modern High-Performance Concrete (HPC) and its adherence to standard codes have enabled longer spans (upto 42m), shallow sections and wider girder spacing (upto 1.56m) by utilizing more efficient pretensioning and posttensioning techniques with low relaxation in HT strands that have been experimentally validated for sufficient loading capacities [15]. The gap here is that the severe deterioration and failures of the first-generation PSC girders are primarily due to a deficiency in shear reinforcement, inadequate grouting leading to corrosion and rupture and the absence of bonded posttensioning systems. Another study investigates the prestress losses for the plate-like concrete bridge structures using the dynamic response [16, 17]. The study describes prefabricated concrete bridge structures, which are analysed using a drop weight impact method and the Finite Element Analysis (FEA) method as a point of comparison [16].

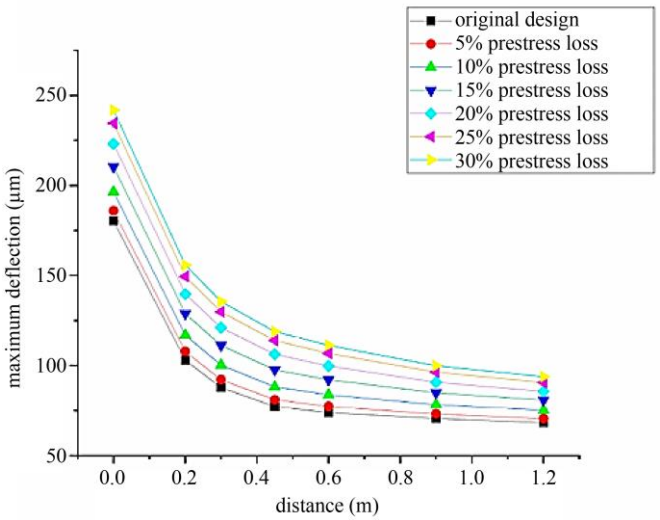

Fig. 2 Bottom plate deflection curve [16]

As shown in Figure 2 above, the key findings concluded that the bottom plate prestressing losses have the most severe impact on the structural stiffness, which is causing around a 33.6% increase in the deflection when the prestress losses reach upto 30% whereas the roof prestress losses have a comparatively minor effect, increasing upto 18.7% [16]. The study limitations are that it remains sensitive to environmental interference and lacks resolution for early-stage damage detection, highlighting the need for more robust and detailed field-applicable techniques. The two-step vibrational method for simultaneously identifying prestress force and unknown excitation in the plate-type concrete bridge structures using only the dynamic responses, concluded that the Load Shape Function (LSF) method [17, 18]. The LSF method effectively determines the moving and the periodic loads with an error of under 10.18% error while the prestress force is identified with an approximate error of 11.32% [17]. A significant gap remains in the method: dependency on the previous knowledge of the loading location and its limited validation under the complex boundary conditions. The study concluded that under the flexural rigidity, experimental prestressing force identification has achieved a maximum relative percentage error of 4.59% and moving force identification with a relative percentage error of 6.52% while the numerical studies showed that the relative percentage error was below 4.01% for the prestressing force and the relative percentage error was 6.09% for the moving force [18]. The current

experimental and numerical analysis are limited to simply supported spans with simulated excitations, highlighting the need for extended applicability to complex boundary conditions. Another research focuses on the adaptation of prestressing methodologies to improve the bridge construction processes. The key findings of the study indicated that the integration of a movable scaffolding system and the application of software like SOFiSTiK for Modelling significantly enhances construction efficiency and stability when employing segmental prestressed beams [19, 20]. Despite these advancements, notable gaps have been found in the existing body of research, particularly in the exploration of long-term performance metrices and the economic implications of implementing these methodologies across diverse bridge structure types and geographic regions. Further investigation in these areas could provide valuable insights for optimizing construction practices and decision-making in civil engineering.

The present research on the prestressing of curved spans in segmental bridges highlights the critical importance of acknowledging the prestressing parameters and carefully designing and executing the prestressing system to ensure bridges' structural stability and longevity. Through a detailed parametric analysis, it is evident that the factors such as curvature radius, tendon profiles, prestressing forces and the tendon elongations significantly influence the overall performance of the bridge throughout its life. Advanced tools like Finite Element Analysis (FEA) have proven to be precious in understanding the complex stress distribution pattern and the optimization in the tendon layout to achieve uniform stress and minimize the local stress concentrations.

2. Methodology

Figure 3 shows the methodology flowchart for the analysis adopted for the present study, and a discussion. The primary methodology is the design parameter identification for the prestressing of a segmental bridge, considering the input data and the tendon layouts, further Modelling and simulating the curve span structure using a finite element method. After the analysis, a construction sequence supported by the parametric analysis is considered to compare what is achieved at the execution of prestressing work. Finally optimizing and concluding the prestressing work to be carried out with the deviation, whether an increase or decrease in the results in terms of prestressing force and Elongation of the HT strands.

2.1. Design Parameter Identifications

The initial step is to identify the design parameter for prestressing of curved spans in segmental bridges. This step involves recognizing and defining the key parametric factors that influence the structural behavior of the bridge and its performance due to prestressing. These parameters include the HT strands layouts which determine the placement and orientation of the prestressing HT bars to ensure uniform distribution of stresses in a longitudinal analysis; the zone of the anchor where the tendons are anchored to the bridge structure specifically the diaphragm segment in case of segmental bridges that affect the load transfer; prestressing forces which needs to be applied accurately in order to balance the structure while maintaining its alignment and radius of curvature which influences the stress distribution of along the span. In order to determine the effective prestressing system, the important factor that governs these situations is the cable profile, including its geometry and alignment.

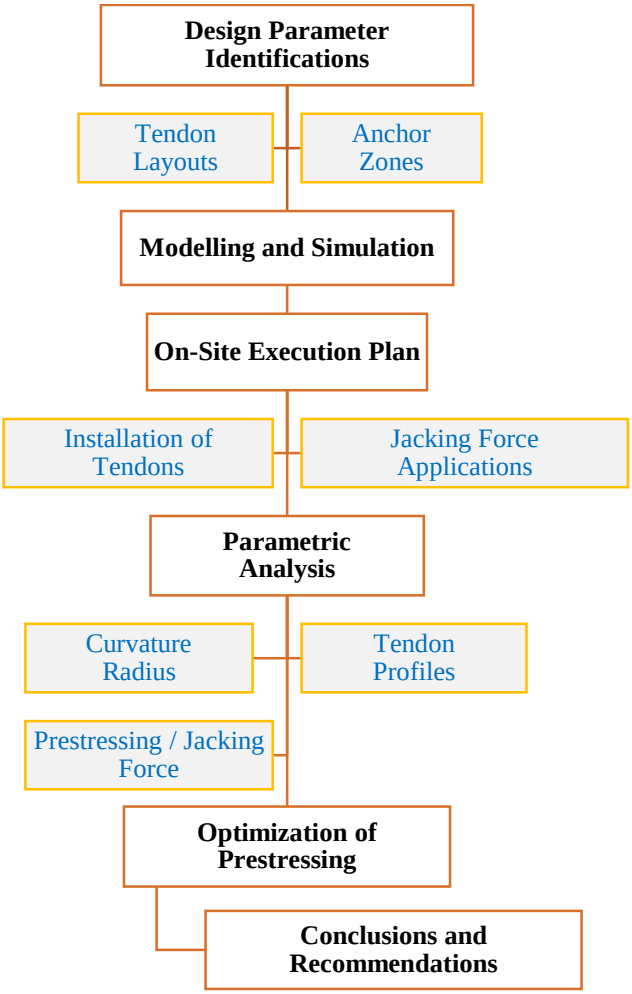

Fig. 3 Methodology flowchart

2.2. Modelling and Simulation

The 3D Modelling tools for the simulation analysis using a Finite Element Method (FEM) are an essential step to understand the behavior of PSC curved spans in segmental concrete bridges. The FEA software, such as Sofistik, Midas and Ansys, enables the formation of detailed 3D models of the bridge structure, which can simulate the complex interactions between the various elements under the different loading conditions. This process begins by defining the geometry of the bridge structure, including the curved span profile, tendon bars, anchor zones, and material properties as required. The

Boundary conditions, such as support reaction and load application points, are later applied to reproduce practical scenarios like dead loads, live loads and other environmental factors. Further meshing is the process of discretizing the structure into small elements, where the FEA tool allows for the precise calculations of stress distribution, strain, deformation and the overall structural response subjected to loading. The generated results provide valuable insights into high stress concentration, bending moments and load transfer mechanisms, helping engineers optimize the prestressing design for enhanced stability, durability and safety. Through iterative simulation techniques, the adjustments carried out to tendon profiles and prestressing forces can be made to achieve the desired performance and ensure the safety and longevity of the bridge structure.

2.3. On-Site Execution Plan

The on-site execution plan for the prestressing of geometric curved spans of a segmental composite concrete bridge needs a well-structured and precise approach to ensure the accurate application of the prestressing forces while maintaining the bridge's structural integrity. The first step is the installation of the prestressing HT tendon bars along the cable ducts or profile, which must be followed as per the predetermined tendon layout or designed during the initial planning phase. The tendons are then placed in ducts within the concrete segments with the utmost careful consideration of the alignment so as to avoid any misplacement, which could affect the overall performance of the bridge structure. Once the tendons are placed, the next step is applying the prestressing forces through the hydraulic jacks. These force applications must be carefully calibrated based on the design specifications to achieve the correct Elongation of the HT bars while also ensuring that the bridge remains properly aligned. Controlled monitoring of the Elongation and jacking force simultaneously during the process is essential, as any deviations from the required values could lead to an improper (excess or deficient) prestressing affecting the structural stability. Adjustments are to be made on-site to account for any of the unforeseen challenges, such as temperature variations, slippage or construction tolerances that may reduce the durability of the bridge structure. Throughout the execution phase, constant supervision and practical measurements are required to track the prestressing process and to ensure adherence to the design requirements. Once the prestressing forces application is complete, the tendons are anchored securely at both ends or one end, depending on the type of prestressing, with one live end or both live ends as per the design. The system needs to be checked for the uniform stress distribution to confirm the effective performance of the prestressing system.

2.4. Parametric Analysis

The Parametric analysis in the background of prestressing in segmental bridges involves systematically varying key design parameters to assess their impact on the structural behavior. This analysis helps identify the most effective combinations of parameters to optimize the performance and ensure stability. The Key parameters are typically examined, including the radius of curvature, tendon profiles, prestressing forces and the tendon bars' elongations. The curvature radius significantly influences the distribution of internal forces and the stresses along the span as it directs the degree of bending and the transfer of loads. The varying tendon profiles allow the evaluation of different tendon geometries and layouts, helping to achieve the uniform stress distribution across the bridge structure while mitigating the local stresses. The prestressing force directly affecting the tension in the tendon bars is another critical factor that must be adjusted to achieve the desired alignment and structural equilibrium. By altering these parameters, one can determine how the variations can affect critical performance metrics such as bending moments, stress variations and the structure's load-bearing capacity. The Parametric analysis typically uses Finite Element Analysis (FEA) to model the bridge behavior under the different configurations, providing insights into how these changes can influence the bridge stability, durability and actual response to the various loading conditions.

2.5. Optimization of Prestressing

The Optimization of prestressing is an important step to ensure a parametric analysis in the framework of prestressing of curved spans in segmental bridges, which involves systematically varying design parameters to assess their impact on the bridge's structural behavior. This analysis helps identify the most effective combinations of the parameters to optimize the performance and ensure stability. Key parameters like the radius of curvature, tendon profiles, prestressing forces and the tendon elongations during the application. The curvature radius significantly influences the distribution of the internal forces and the stresses along the span, as it directs the degree of bending and the load transfer mechanism. The varying tendon profiles allow the evaluation of different tendon geometries and layouts, helping to achieve uniform stress distribution across the bridge while mitigating the local stresses. The prestressing force, which directly affects the tension force in the tendon bars, is another critical factor that must be adjusted to achieve the desired alignment and structural equilibrium. This process ensures that the optimal prestressing force in design is adopted to achieve the necessary structural performance with minimum risk of deficiencies.

2.6. Prestressing Parameters

The design prestress formulas are used to determine the optimal amount of prestressing force required to counteract the applied loads on the structure and maintain its desired shape and stability. These formulas typically involve calculation of the required jacking force, tendon elongations, modified elongations and the distribution of stresses within the concrete to achieve a balanced and effective design. The prestress force is applied to induce compressive stresses in the

concrete to compensate for the tensile stresses caused by the external loadings. The formulas that account for various parameters include the material properties, tendon geometry, curvature of the span and the external loads to ensure that the prestressed concrete structure performs optimally while minimizing the risk of any excessive deformation, further leading to the structure's cracking or failure. The revised elongation calculation depends on the original Elongation and the new modulus as given in Equation (1). The new Elongation relies on the grip length calculated using Equation (2). Modified gauge pressure is directly proportional to the jacking force and inversely proportional to the jack efficiency calculated as given in Equation (3). The modified Elongation is the ratio of theoretical values to the actual values measured at the site, given in Equation (4).

$$\text{Rev. Elongation} = \frac{(1.95 \times 10^5) \times \text{Original Elongation}}{\text{New Modulus}} \times \frac{140}{\text{New Area}} \quad (1)$$

$$\text{New Elongation} = \text{E}_X + \left(\frac{\text{Jack Force} \times 10000}{\text{Tension Area} \times \text{E}}\right) \times \text{Grip Length} \quad (2)$$

$$\text{Modified Gauge Pressure} = \frac{\text{Jacking Force}}{\text{Jack Ram Area} \times \text{Jack Efficiency}} \quad (3)$$

$$\text{Mod. Elongation} = \frac{\text{Th. Elongation} \times \text{Th. Elastic Modulus} \times \text{Th. Area}}{\text{Actual Elastic Mudulus} \times \text{Actual Area}} \quad (4)$$

3. Input Parameters and Boundary Conditions

The proposed design parameters for the bridge structure include a superstructure constructed using high-strength concrete of grade M55, ensuring the durability and the structural performance under heavy loadings and dynamic conditions. The grade of reinforcement steel specified is Fe500D, which provides high ductility and strength, making it suitable for handling the stresses imposed by the bridge's operational and environmental demands. The 19T15 cable type was chosen for the prestressing system and was designed to handle the dynamic prestress effectively. These cables are strategically integrated into the structure to enhance its load-carrying capacity, minimize deflections, and counteract the concrete's tensile stresses. Table 1 illustrates the required input parameters and the material properties considered for the analysis.

Table 1. Input data for the material properties

Description	Value
Concrete Grade	M-50
Unit Weight of Concrete (γ_c)	25 kN/m³
Grade of Reinforcing Steel	Fe-500
Unit Weight of Steel (γ_s)	7850 Kg/m³
Steel Elastic Modulus (E_s)	200,000 N/mm^2
Type of Anchorage	19 T 15
Slip at each end	6 mm
Coefficient of friction μ	0.17 / rad
Wobble coefficient k	0.0020 / m
Modulus of elasticity of HT-Steel	195,000 N/mm^2

4. Design Parameters

As per the IRC:6 Clause 204.4 [22], under the "Congestion Factor" condition, the horizontal forces resulting from braking or acceleration, centrifugal action, temperature effects and the effects of the transverse eccentricity of live loads are excluded. Further, it specifies that the congestion factor does not apply to the load combinations involving the case of Special Vehicle (SV) loading [22].

The stressing operations are to be carried out in two stages, followed by the stage construction sequence. The anchorage system so considered is of 19T15. The concrete's stage-1 stressing shall be carried out on the 28th day to achieve full strength while performing the stressing operations. The other prestressing losses, such as anchorage slip, dead-end slip, loss due to friction, creep, shrinkage, elastic shortening, and relaxation of steel, are considered as per IRC standards. The check for the flexural stress is performed under the condition of the limit state of the serviceability conditions. The Prestressing Factors of 1.1 & 0.9 are considered as per clause 7.9.5 of IRC:112-2011 [23]. The Moment of Resistance and Shear Capacity checks are applied at the Ultimate Limit State (ULS) for a prestressing factor of 1.0 per clause 7.9.5 of IRC:112-2011 [23]. Further Suitable load factors are considered for each limit state condition as required.

The minimum number of cables to be stressed before moving the auto-launching girder has been calculated, and the corresponding calculations are presented in this design as a "check for launching condition". In this check, in addition to the self-dead weight of the spine beam, the launcher loads, and the live load are taken as 50 kg/m^2 as per Annexe-06 of IRC:112. Prestressing effects may be taken as $\gamma = 1$ during the construction as per the same annexure [23]. It is noted that a minimum of cable ducts are to be stressed before moving the launching girder ahead, and which particular cables are to be stressed is presented in these design calculations. Eccentric loading of live load on the spine beam and curvature effects due to self-weight, SIDL loads and live loads cause pure Torsion and the differential bending of the top and the bottom slabs. Differential bending of top and bottom slabs causes longitudinal warping and transverse distortion of the spine beam. The Distortional Analysis is done based on "Beam on elastic foundation Analogy" as suggested by Derrick Beckett [24]. The longitudinal warping stresses are also considered in the design. The distortional bending moments due to curvature are also calculated, and the effect is also considered in this design in both SLS and ULS limit states.

Table 2 shows the cable profile, and Table 3 shows the jacking force needed to be applied along with the corresponding elongations calculated as per the design. A 6mm slip is also considered in the design, which will be measured as actual during further application of the stressing operations. The jacking force is given in metric tonnes, where 26 cables are to be stressed with the suitable sequences.

Table 2. Cable profile

Cable	a *(m)*	b *(m)*	c *(m)*	d *(m)*	H *(m)*	h3 *(m)*
1	1.325	15.0	0	3.000	2.180	0.8875
2	1.325	15.0	0	3.000	1.740	0.6375
3	1.325	15.0	0	3.000	1.300	0.3875
4	1.325	15.0	0	3.000	0.860	0.1375
5-5	1.000	1.5	0	16.975	0.276	0.1390
6-6	1.000	1.5	0	16.975	0.283	0.1460
7-7	1.000	1.5	0	16.975	0.296	0.1590
8-8	1.325	15.0	0	3.000	2.440	1.5830
9-9	1.325	15.0	0	3.000	2.011	1.3390
10-10	1.325	15.0	0	3.000	1.581	1.0940
11-11	1.325	15.0	0	3.000	1.151	0.8500
12-12	1.000	1.5	0	16.975	0.721	0.6060
13-13	1.000	1.5	0	16.975	0.654	0.5150
14-14	1.000	1.5	0	16.975	0.593	0.4540
15-15	1.000	1.5	3	13.975	0.537	0.4160

Table 3. Jacking force and elongations

Cable	Ducts *(Nos.)*	Jacking force *(t)*	Elongation *(mm)*
1	1	395.36	280.76
2	1	395.36	281.03
3	1	395.36	281.34
4	1	395.36	281.71
5-5	2	395.36	282.30
6-6	2	395.36	282.30
7-7	2	395.36	282.30
8-8	2	270.51	281.45
9-9	2	395.36	281.81
10-10	2	395.36	282.22
11-11	2	395.36	282.67
12-12	2	395.36	282.83
13-13	2	395.36	282.26
14-14	2	395.36	282.26
15-15	2	395.36	276.49

As mentioned, the Jacking force for each strand's profile is in metric tons of force to be applied at the jacking end. The Elongation achieved with respect to each strand is calculated separately as per the requirement shown in Table 3. Figures 4, 5, and 6 are read together along with Table 2 and Table 3. Figure 2 is the geometric arrangement for profiling the HT strands, where the values shown in Table 2 for columns a, b, c, and d are the distances illustrated corresponding to Table 3 for each cable/duct nos.

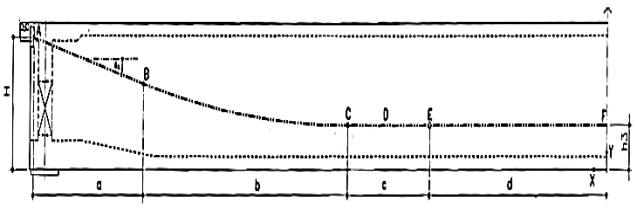

Fig. 4 Geometric profiling

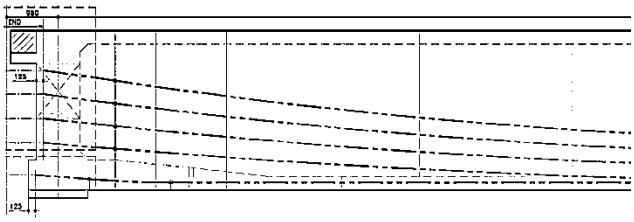

Fig. 5 HT Strands profile in outer web and inner web

As per Figure 5, the HT strand profiling was drafted in CAD for the outer and the inner web portion corresponding to the duct nos shown in the cross section illustrated in Figure 6 below. Figure 5 shows the parabolic profile for the HT-strands laid corresponding to the.

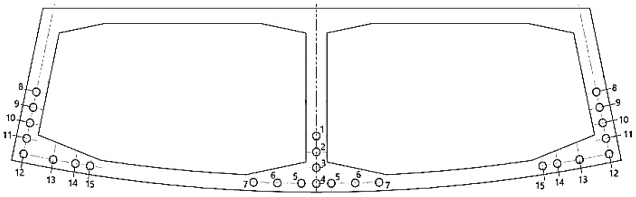

Fig. 6 HT strands ducting numbers in segment cross-section

Figure 6. The repetition of the numbers in the cross-section for Figure 6, corresponding to Table 2, indicates the same profile and the same force needed to be applied simultaneously at the jacking end while performing the prestressing operations.

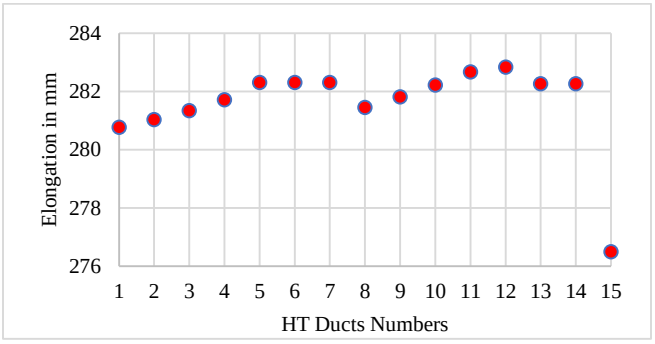

Fig. 7 Calculated Elongations for each Duct

Figure 7 above represents the graphical representations of the elongations required for each duct while stressing. The graph shows that each duct needs different elongations based on its profile and eccentricity from the neutral axis. The general methodology adopted by the design engineers is to calculate an average elongation by calculating the average jacking force for each duct.

4.1. The Construction Sequence

The construction process for segmental bridges involves a systematic sequence to ensure precision and stability. Initially, the spine beams are cast in the precast yard, transported to the site, and erected using an overhead launching girder at their designated positions. These beams are temporarily placed on bearings, and longitudinal prestress is applied in two stages to achieve structural alignment. Simultaneously, wing sections are cast in the precast yard, transported, and connected to the spine beams using cast-in-situ concrete stitches, ensuring proper integration. Finally, prestressing is applied to the wings to enhance overall stability. The detailed steps are as follows:

- Casting of spine beams in the precast yard and transporting them to the site.
- Erecting the spine beams in their respective positions using an overhead launching girder.
- Placing spine beams on temporary bearings and applying longitudinal prestress in two stages:
  - The first stage is with the launching girder.
  - Second stage without the launching girder.
- Casting wing sections in the precast yard and transporting them to the site.
- Lifting the wings with gantry girders, connecting them to the spine beams through cast-in-situ concrete stitches, and joining adjacent wings similarly.
- Applying prestress to the wings to ensure structural stability and integration.

5. Results and Discussion

This section discusses the result obtained for the analysis carried out using an FEA-based tool and the stress result obtained after applying the prestressing force to the segmental section.

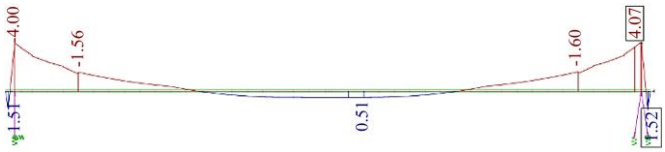

Fig. 8 Stress value of spine beam at top fibre due to prestress

Figure 8 shows the stress value in the top fibre due to prestress after performing the analysis using the FEA model. In the longitudinal analysis for the stressing operations, the maximum negative value obtained is -4.07 N/mm^{2,} while the maximum positive value is around 1.52 N/mm^2.

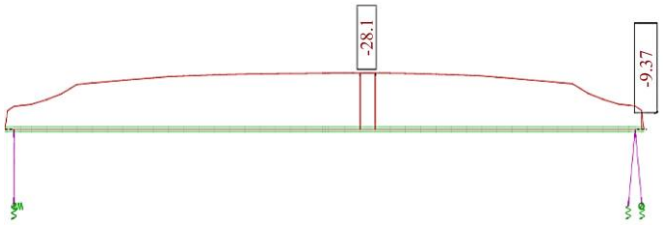

Fig. 9 Stress value of spine beam at the bottom fibre due to prestress

Similarly, Figure 9 shows the stress in the bottom fibre due to prestress in the spine beam, which is around -28.1 N/mm^2 near the middle and -9.37 N/mm^2 at the supports.

The Figure 6 below shows the total stresses of the full span considering the spine beam conditions, where the maximum negative value is found in the middle of the span, around -5.80 N/mm^2. Meanwhile, the support is -4.06 N/mm^2 and positive 1.52 N/mm^{2,} respectively.

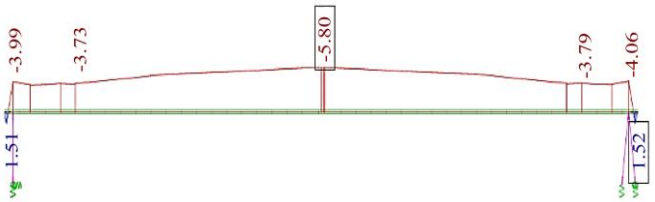

Fig. 10 Total stresses in the top fibre (only spine beam condition)

Similarly, from Figure 10 of the total stress diagram, when the full spine beam is activated, the actual and maximum stress value so obtained is around -21.33 N/mm^2, -21.14 N/mm^2 and -21.69 N/mm^2 at the middle portion of the span.

As per IRC 112, the maximum allowable compressive stress is 0.48fck, which equals around 24 N/mm^2 for the concrete grade of M50. Now this value is very close to the allowable compressive stress in the concrete.

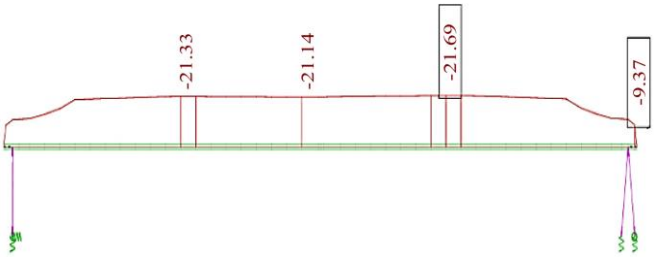

Fig. 11 Total stresses in the bottom fibre (only spine beam condition)

While considering the revised code regarding the amendment issued on 01 Oct 2023 on IRC: SP:65 2018 Guidelines for Design and Construction of Segmental Bridges (First Revision) [25], the maximum compressive stress is to be limited to 0.36fck (i.e. 0.36 x 50 = 18 N/mm^2).

This amendment was released after the design stage; however, this point is important for the maximum compressive stress in concrete to be allowed. Hence, for such a case, the structure stress exceeds the limiting value as per the revised codal amendments.

The data shown in Table 4 below for the modified and new Elongation is generated by using the Equations (1), (2), (3), and (4) mentioned above in the methodology. After performing the stressing operations at the site, the values of the extension are achieved for each of the ducts mentioned separately, along with the actual measured slip at the site.

Table 4. Net elongations data

Cable No	Applied Pressure	Th. extension	Modified extension	Extension achieved	Net Extension	Percent change
	Kg / cm²	*mm.*	*Mm.*	*Mm.*	*Mm.*	
1	382	278	281.09	288.60	282.60	0.54%
9 L	382	280	283.43	290.00	284.00	0.20%
9 R	382	280	283.43	286.00	284.00	0.20%
2	382	278	281.08	287.67	281.67	0.21%
3	382	279	282.10	286.66	280.66	-0.51%
10 L	382	281	284.00	298.33	292.33	2.93%
10 R	382	281	284.00	288.30	282.30	-0.60%
4	382	280	283.10	297.00	291.00	2.79%
11 L	382	282	285.29	289.33	283.33	-0.69%
11 R	382	282	285.29	300.67	294.67	3.29%
5 L	382	282	285.12	291.66	285.66	0.19%
5 R	382	282	285.12	295.66	289.66	1.59%
13 L	382	282	285.12	295.00	289.00	1.36%
13 R	382	282	285.12	294.00	288.00	1.01%
6 L	382	282	285.13	290.33	284.33	-0.28%
6 R	382	282	285.13	299.30	293.30	2.87%
14 L	382	282	285.13	293.00	287.00	0.66%
14 R	382	282	285.13	289.33	283.33	-0.63%
7 L	382	282	285.12	300.33	294.33	3.23%
7 R	382	282	285.12	297.66	291.66	2.29%
15 L	382	282	285.13	296.00	290.00	1.71%
15 R	382	282	285.13	299.00	293.00	2.76%
12 L	382	283	286.13	292.00	286.00	-0.05%
12 R	382	283	286.13	290.00	284.00	-0.74%
8 L	261	279	282.10	290.50	284.50	0.85%
8 R	261	279	282.10	290.00	284.00	0.67%

From the values shown in Table 4 above, the maximum variation of 3.29 percent is observed on duct no. 11 to the right-hand side, where the elongation value so obtained is around 294.67 mm net and that with the 4mm of slip is also observed at one end during the stressing operations.

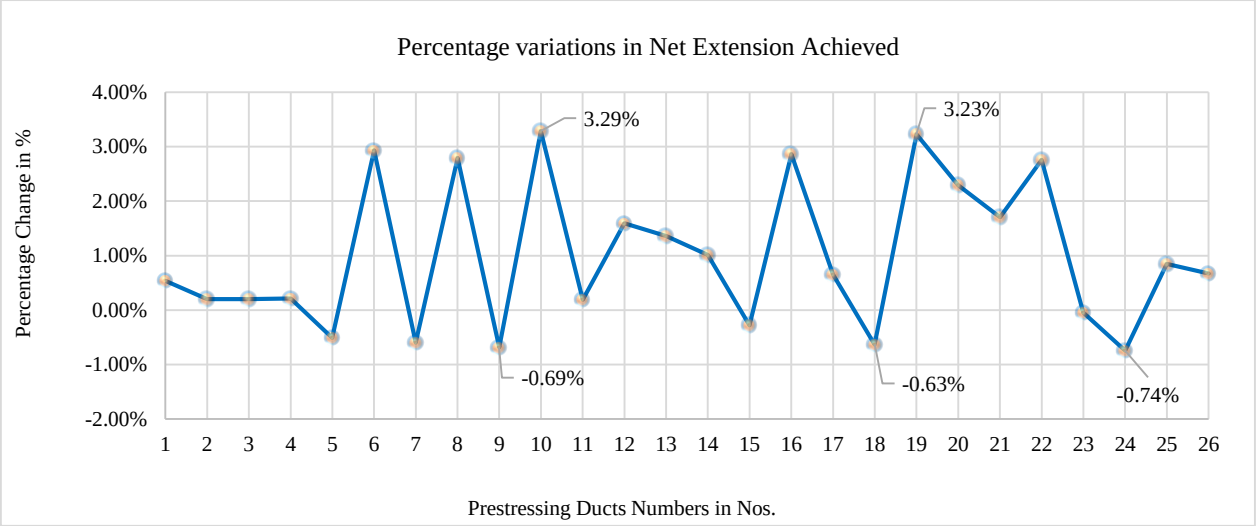

Fig. 12 Percentage variations in the net-extensions of HT strands

Figure 12 illustrates the graphical representation of the variations in net extension observed with respect to the calculated extension for the curved span with a radius of curvature upto 300m. The data reveals that the maximum negative variation in net extension is -0.74%, indicating a slight reduction compared to the expected value. Conversely, the maximum positive variation is around 3.29% reflecting a noticeably higher variation in net Elongation of the HT strands. These variations highlight the influence of the span's curvature on the cable extensions and emphasize the need for an accurate consideration of plan geometry in the analysis.

Figure 13 shows the comparison between the theoretical elongations calculated and actual elongations achieved during the stressing operations of HT strands across 26 ducts. Four sets of values are compared: theoretical extension, modified extension, extension achieved and net extension achieved for the HT strands. It is further observed that the theoretical extensions remain nearly constant at around 278mm to 282 mm for all ducts, as shown by the blue line. Further, after incorporating the practical corrections, the modified extensions represented by the green line are slightly on the higher side, ranging from about 282mm to 285 mm. This indicates the allowance made for the site conditions and the material variations. In contrast, the achieved elongations represented by the orange line are significantly higher and fluctuate between 287mm and 301 mm. These values consistently exceed the theoretical predictions, showing

variations due to the practical factors such as frictional losses, anchorage slip and handling at the site. The maximum achieved Elongation was about 300.67 mm at Duct No.10 and Duct 19, while the minimum was around 287 mm for Duct No. 3.

The net Elongation achieved after deducting the actual slip is represented by the purple line, which lies between the modified and achieved ones, with the values ranging between 290mm and 295 mm for most ducts. Although closer to the achieved elongations, they still reflect the considerable variation when compared with the theoretical elongation lines. Also, the trends of both achieved elongations are similar. Overall, the results show that the achieved elongations are consistently higher than the theoretical and modified values. The variation highlights the difference between the calculated assumptions and the field conditions. This deviation, though present, remains within acceptable tolerances (±5%) as per the standard prestressing practices. The data confirms that elongation control is a reliable method for stress verification, but site corrections and practical monitoring are essential to ensure the accuracy of prestressing systems.

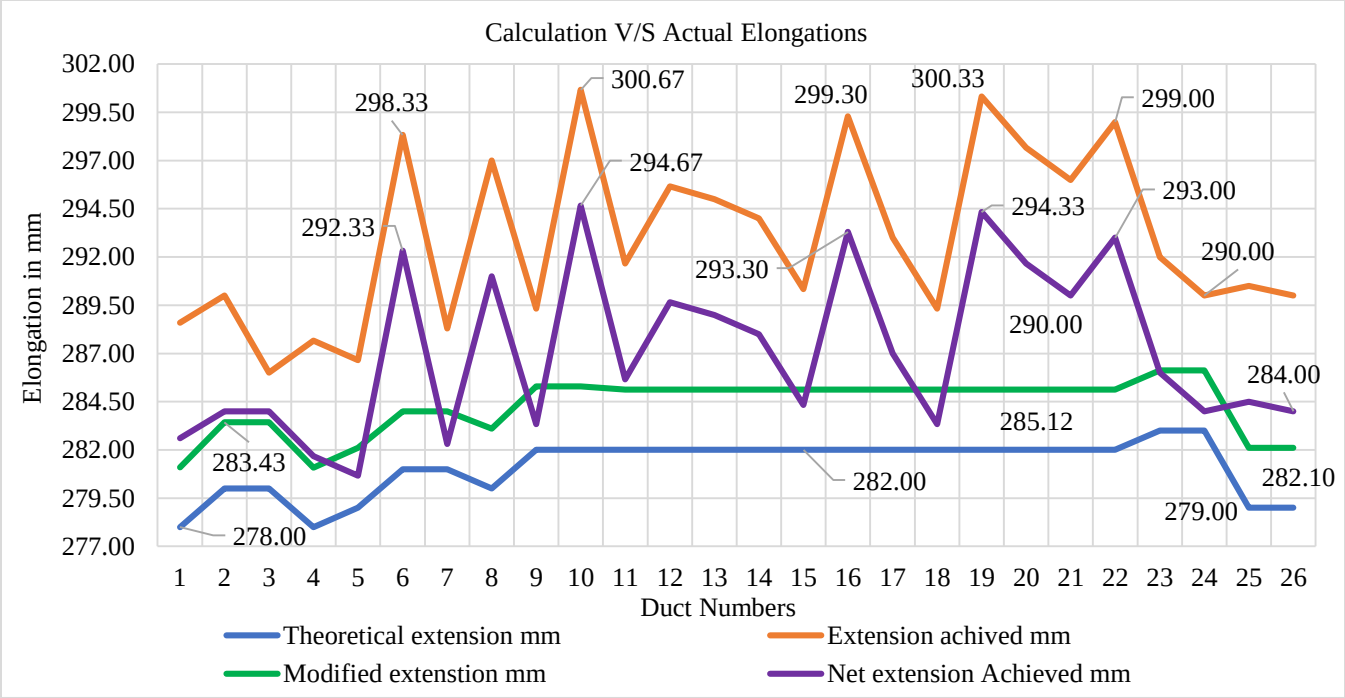

Fig. 13 Theoretical Versus Actual elongations of the HT strands

The curvature of cables in the plan geometry is typically not accounted for in the slip loss analysis. As a result, the cable lengths are often assumed to be the same as those of the central web cables, even for the outer and inner web portions. This assumption can lead to deficiencies in the calculated forces, as the extensions at actual or as per the design may not represent the true forces. The study also underscores the challenges faced during on-site execution, emphasizing the need for precise alignment and controlled monitoring of the jacking forces to ensure an accurate prestressing and structural equilibrium.

6. Conclusion

The difference in lengths between the outer and inner web cables results in the cables in the inner web being overstressed by a factor of 1.055. For instance, the measured extension is 268 mm when considering the plan curvature of the cables and the profile provided, as compared to 283 mm shown. According to IRC 112 Clause 7.9.2, under exceptional conditions, the maximum allowable overstressing during prestressing operations is 95% of 0.1% proof load or proof stress, which equals 0.87 × 0.95 = 0.826 times the ultimate tensile strength (UTS). The stressing operation for both stages, with all cables prestressed in an ungrouted condition, was simulated using a simulation tool. The strength of the concrete was verified against the specified value of 50 MPa in the drawings. As per IRC 112, the maximum allowable compressive stress is 0.48fck, which equates to 24 MPa (i.e., 0.48 × 50 MPa). Under the dead load (Spine Beam) and full prestressing with ungrouted cables, the maximum compressive stress at the bottom fibre was observed to be 21.36 MPa, without overstressing the cables as previously discussed. However, when simulating cable stressing based on the extensions provided in the drawing, the stress at the bottom fibre increased slightly to 21.69 MPa, remaining within permissible limits. By addressing these areas, future projects involving curved spans in segmental bridges can achieve

optimal performance, reduced maintenance costs, and enhanced safety, ensuring that they meet the evolving demands of modern infrastructure.

Acknowledgments

All authors contributed equally to the preparation of this article.

References

[1] Cong Ye et al., "Evaluating Prestress Losses in a Prestressed Concrete Girder Railway Bridge Using Distributed and Discrete Fibre Optic Sensors," *Construction and Building Materials*, vol. 247, 2020. [CrossRef] [Google Scholar] [Publisher Link]

[2] Liam J. Butler et al., "Evaluating the Early-Age Behaviour of Full-Scale Prestressed Concrete Beams Using Distributed and Discrete Fibre Optic Sensors," *Construction and Building Materials*, vol. 126, pp. 894-912, 2016. [CrossRef] [Google Scholar] [Publisher Link]

[3] Terry Y.P. Yuen et al., "DFEM of a Post-Tensioned Precast Concrete Segmental Bridge with Unbonded External Tendons Subjected to Prestress Changes," *Structures*, vol. 28, pp. 1332-1337, 2020. [CrossRef] [Google Scholar] [Publisher Link]

[4] Jr. Walter Podolny, "An Overview of Precast Prestressed Segmental Bridges," *PCI Journal*, vol. 24, no. 1, pp. 56-87, 1979. [CrossRef] [Google Scholar] [Publisher Link]

[5] Walter Podolny, and Jean M. Muiler, *Construction and Design of Prestressed Concrete Segmental Bridges*, Wiley, pp. 1-561, 1982. [Google Scholar] [Publisher Link]

[6] S.K. Padmarajaiah, and Ananth Ramaswamy, "A Finite Element Assessment of Flexural Strength of Prestressed Concrete Beams with Fiber Reinforcement," *Cement and Concrete Composites*, vol. 24, no. 2, pp. 229-241, 2002. [CrossRef] [Google Scholar] [Publisher Link]

[7] Antonio F. Barbosa, and Gabriel O. Ribeiro, "Analysis of Reinforced Concrete Structures Using Ansys Nonlinear Concrete Model," *Computational Mechanics*, pp. 1-7, 1998. [Google Scholar]

[8] Nimiya Rose Joshuva et al., "Finite Element Analysis of Reinforced and Pre-Tensioned Concrete Beams," *International Journal of Emerging Technology and Advanced Engineering*, vol. 4, no. 10, pp. 449-457, 2014. [Google Scholar]

[9] Muhammad Aslam et al., "Strengthening of RC Beams Using Prestressed Fiber Reinforced Polymers – A Review," *Construction and Building Materials*, vol. 82, pp. 235-256, 2015. [CrossRef] [Google Scholar] [Publisher Link]

[10] A.G. Razaqpur, Mostafa Nofal, and M.S. Mirza, "Nonlinear Analysis of Prestressed Concrete Box Girder Bridges under Flexure," *Canadian Journal of Civil Engineering*, vol. 16, no. 6, pp. 845-853, 1989. [CrossRef] [Google Scholar] [Publisher Link]

[11] Amorn Pimanmas, "The Effect of Long-Term Creep and Prestressing on Moment Redistribution of Balanced Cantilever Cast-Inplace Segmental Bridge," *Songklanakarin Journal of Science and Technology*, vol. 29, no. 1, pp. 205-216, 2007. [Google Scholar] [Publisher Link]

[12] Yanwei Niu, and Yingying Tang, "Effect of Shear Creep on Long-Term Deformation Analysis of Long-Span Concrete Girder Bridge," *Advances in Materials Science and Engineering*, vol. 2019, no. 1, pp. 1-10, 2019. [CrossRef] [Google Scholar] [Publisher Link]

[13] Srushti D. Somkuwar, and Amey Khedikar, "A Parametric Study of Curved Prestressed Concrete Box Girder," *International Journal of Creative Research Thoughts*, vol. 9, no. 3, pp. 2080-2098, 2021. [Publisher Link]

[14] Barbaros Atmaca, "Determination of Minimum Depth of Prestressed Concrete I-Girder Bridge for Different Design Truck," *Computers and Concrete*, vol. 24, no. 4, pp. 303-311, 2019. [CrossRef] [Google Scholar] [Publisher Link]

[15] Petra Bujňáková, and Miroslav Strieška, "Development of Precast Concrete Bridges during the last 50 Years in Slovakia," *Procedia Engineering*, vol. 192, pp. 75-79, 2017. [CrossRef] [Google Scholar] [Publisher Link]

[16] Jilei He et al., "Analysis of the Prestressing Loss Influence in Prefabricated Concrete Bridges Based on a Drop Weight Impact Method," *Buildings*, vol. 14, no. 12, pp. 1-14, 2024. [CrossRef] [Google Scholar] [Publisher Link]

[17] Wensen Wang et al., "Prestress Force and General Excitation Identification for Plate-like Concrete Bridges," *Buildings*, vol. 14, no. 7, pp. 1-19, 2024. [CrossRef] [Google Scholar] [Publisher Link]

[18] Kunaratnam Jeyamohan et al., "Prestress Force and Moving Force Identification in Prestressed Concrete Bridges via Lagrangian Polynomial-Based Load Shape Function Approach," *Journal of Civil Structural Health Monitoring*, vol. 15, pp. 575-596, 2025. [CrossRef] [Google Scholar] [Publisher Link]

[19] Goran Markovski , and Marija Docevska, Adaptation of the Prestressing Methodology to the Bridge Construction Method, Proceedings of the Conference on Structural Engineering, 2022. [Online]. Available: https://www.researchgate.net/publication/360307047_Adaptation_of_the_prestressing_methodology_to_the_bridge_construction_method

[20] Sofistik Structural Analysis Software Documentation, Sofistik AG., Oberschleißheim, Germany, 2020, [Online]. Available: https://www.sofistik.com/fileadmin/user_upload/Products/Highlights_V2020/New_Features_SOFiSTiK_2020_en.pdf

[21] "*Specifications for Road and Bridge Works*," Report, Ministry of Road Transport and Highways, Indian Roads Congress, pp. 1-906, 2013. [Publisher Link]

[22] "*IRC 6: 2017, Standard Specifications and Code of Practice for Road Bridges*," Indian Roads Congress, pp. 1-122, 2017. [Publisher Link]

[23] "*IRC: 112-2020, Code of Practice for Concrete Road Bridges*," Indian Roads Congress, pp. 1-256, 2020. [Publisher Link]

[24] Derrick Beckett, *An Introduction to Structural Design: Concrete Bridges*, Surrey University Press, vol. 1, pp. 1-228, 1973. [Publisher Link]

[25] "*IRC: SP: 65: 2018, Guidelines for Design and Construction of Segmental Bridges*," Indian Roads Congress, pp. 1-28, 2018. [Publisher Link]

[26] "*IRC: 18-2000, Design Criteria for Prestressed Concrete Road Bridges (Post-Tensioned Concrete)*," Indian Roads Congress, pp. 1-38, 2000. [Publisher Link]